Limitations of the friction model of low-energy electronic stopping

Sigmund, Peter; Schinner, Andreas

Published in:
Nuclear Instruments and Methods in Physics Research Section B: Beam Interactions with Materials and Atoms

DOI:
10.1016/j.nimb.2022.10.023

Publication date:
2023

Document version:
Accepted manuscript

Document license:
Unspecified

Citation for pulished version (APA):
Sigmund, P., & Schinner, A. (2023). Limitations of the friction model of low-energy electronic stopping. *Nuclear Instruments and Methods in Physics Research Section B: Beam Interactions with Materials and Atoms*, *534*, 39-44. https://doi.org/10.1016/j.nimb.2022.10.023

Limitations of the Friction Model of Low-Energy Electronic Stopping

Peter Sigmund[a], Andreas Schinner[b]

[a]*Department of Physics, Chemistry and Pharmacy, University of Southern Denmark, DK-5230 Odense M, Denmark*
[b]*Department of Experimental Physics, Johannes Kepler University, A-4040 Linz, Austria*

Abstract

This is a follow-up on three recent studies of the significance of impact-parameter-dependent electronic energy loss in the stopping of low-energy ions in matter [1, 2, 3]. With reference to the friction model of electronic stopping we distinguish between two deviations from velocity-proportional stopping, i.e., RM corrections – which account for nonuniform projectile motion during collisions – and RED corrections which account for the influence of the detector geometry on the output signal. With the emphasis on RM corrections we study gas and solid targets and, in particular, conductor-insulator differences as well as projectile-isotope effects. An important aspect is the interference between RM and RED corrections, which was left out in our previous study [3]. Here we find that the combined action of the two corrections is *smaller* than the RM correction.

Keywords: Electronic stopping, nuclear stopping, impact-parameter-dependent energy loss, conductor-insulator difference, isotope effect

1. Introduction

Energetic ions slow down in matter due to interaction with the electrons and nuclei of the stopping medium. Early studies of this topic, dating back to more than a century ago [4], addressed the penetration of alpha particles in the MeV energy range, where the stopping force is determined primarily by interaction with the electrons in the target, whereas the target nuclei are responsible for angular deflection (Rutherford scattering).

This scheme is very successful and still the standard for dealing with high-energy light particles. However, an expansion was needed after the discovery

Email address: sigmund@sdu.dk (Peter Sigmund)

Table 1: The LSS scheme in the interaction of ions with matter. $d\sigma_n$ denotes the elastic scattering cross section vs. energy transfer T_n to the target nucleus or vs. scattering angle ϕ of the ion. $S_e(E)$ denotes the electronic stopping cross section vs. energy E of the ion.

Interaction with:	Target nuclei	Target electrons
Energy transfer:	$d\sigma_n(T_n)$	$S_e(E)$
Deflection:	$d\sigma_n(\phi)$	ignored

of nuclear fission, because fission products, i.e., heavy ions in the upper-keV/u energy range, experience significant energy loss also to the target nuclei [5].

Table 1 illustrates a very successful scheme, established by Lindhard et al. [6, 7, 8] and covering potentially all ion-target combinations and a wide range of beam energies. The scheme implies that

I Energy transfer to nuclear and electronic stopping is treated as separate processes,

II Electronic stopping is treated as a friction force defined by a stopping cross section $S_e(E)$,

III Nuclear stopping and scattering are characterized by a differential cross section $d\sigma(E, T_n)$ or $d\sigma(E, \phi)$ for elastic scattering.

This package has, in the original as well as numerous modified versions, provided a successful basis for ion beam physics over the past sixty years via theoretical and simulational treatments of ionization phenomena, ion implantation and ion-beam analysis, radiation damage, and emission processes like sputtering and electron emission.

There are a number of missing effects, the most prominent of which being the expression for the friction force which, in the original form, only covered the energy range below the Bragg peak. This was handled as soon as the scheme was applied to higher beam energies [9].

Another lack, still missing in most treatments, is the neglect of fluctuations in electronic energy loss (straggling), even though knowledge of straggling has greatly expanded recently [10].

The present study is devoted to two items that have in common that

- they go beyond the friction model for electronic stopping,
- become significant mainly at beam energies below ~ 20 keV/u, and
- involve the mass – and not only the charge – of the projectile nucleus.

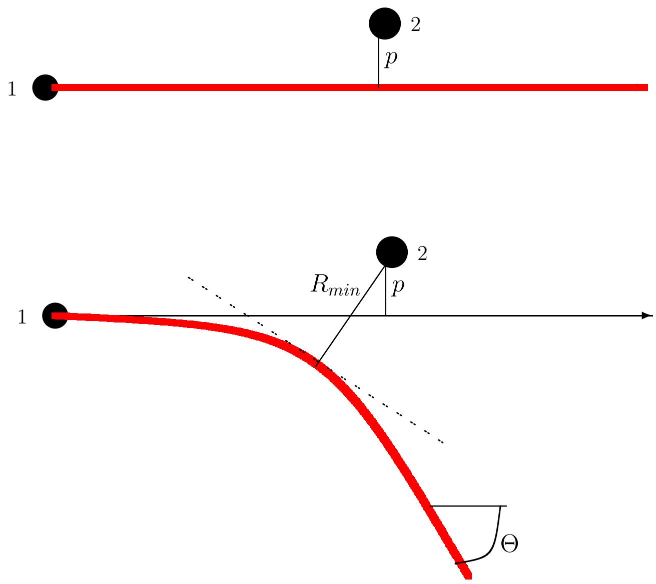

Figure 1: Upper graph: Standard trajectory in stopping theory. Lower graph: Taking into account deflection under collision.

Regarding points I-III above, consider the interaction between an ion and a target atom or molecule. Conservation laws require that both, electrons and nuclei are scattered, although their relative contributions to energy loss and deflection depends on the participating species and energy. While this coupling between electronic and nuclear interactions is ignored in the LSS model, it may be taken into account within the spirit of the model by incorporating the impact-parameter dependence of the electronic energy loss. In this context, the impact parameter p denotes the distance between a straight-line trajectory and a target *nucleus*, thus allowing for either a quantal or classical description of the ion-electron interaction.

In a recent study [3] we have demonstrated that ignoring the deflection of the projectile *during* a collision – a standard approximation in stopping theory – can be a major source of error. Incorporation of this effect into the PASS code [11] showed a significant influence on the stopping cross section at energies below $\sim$ 20 keV/u.

We have also studied the influence of impact-parameter-dependent electronic stopping on the analysis of stopping measurements in transmission [1] and reflection [2].

Main consequences of our treatment are necessary corrections to tabulated stopping cross sections such as DPASS [12] and CasP [13, 14], insulator-metal differences and isotope differences in electronic stopping. In the present study we follow up on consequences of the RM correction, i.e., deviation from a pro-

Table 2: Definition of modifications to standard stopping theory.

Notation	p_{eff}	E_{eff}
RM0	p	E_0
RM1	$R_{\min}$	E_0
RM2	$R_{\min}$	$E_0 - V(R_{\min})$

jectile in uniform motion, in particular on conductor-insulator difference and isotope effect, and the validity of published stopping tables, as well as the combined action of RM and RED corrections.

2. Recapitulation

The upper graph in Figure 1 illustrates the standard description of the collision geometry in stopping theory as introduced by Bohr [4] and Bethe [15] and followed in numerous theoretical and numerical schemes to estimate electronic energy loss, notable exceptions being discussed below. The essence is uniform motion of the projectile during passing by a stationary target atom ('sudden approximation').

The lower graph illustrates an approximation introduced by Firsov [16], where the actual trajectory, indicated by the red line, is replaced by a straight line going through the point of closest approach. An improved estimate of the stopping cross section, called RM1 in the following, is then obtained by running PASS – or another stopping theory incorporating the equivalent of an impact parameter – by replacing the impact parameter by the distance of closest approach $R_{\min}$, which is defined by [17]

$$1 - \frac{V(R_{\min})}{E_{\text{rel}}} - \frac{p^2}{R_{\min}^2} = 0.$$

Actually, the projectile undergoes a change in kinetic energy during collision. To account for this, we introduce an additional correction by subtracting the change in potential energy $V(R_{\min})$ at the point of closest approach from the beam energy. The combined result of the change in impact parameter and beam energy will be called RM2 approximation in the following. Ignoring both changes, i.e., the approximation underlying standard stopping theories, has been denoted as RM0 (table 2).

We want to emphasize that the use of realistic trajectories is well established in atomic-collision theory. In the description of ion-induced x-ray emission the effect is known as Coulomb deflection [18].

The replacement of the impact parameter by the distance of closest approach is an important aspect of Firsov's [16] formula for $T(p)$. However, when applied to estimate stopping cross sections the standard procedure [19] has been to neglect this step. This has resulted in the generally expressed, but incorrect view that Firsov's formula would predict velocity-proportional stopping.

A more adequate evaluation of stopping cross sections on the basis of Firsov theory was presented by Karpuzov [20].

An alternative approach was presented by Semrad [21], who demonstrated, on the basis of measured inner-shell excitation cross sections, that Coulomb deflection is influential in the stopping of low-energy ions. Semrad also presented theoretical estimates on the basis of electron-gas theory [22, 23] in conjunction with a local-density approximation.

3. Conductor-Insulator Difference

In the following, computations on electronic stopping by bound electrons have been performed by the PASS code in the version underlying ref. [3], whereas stopping by free electrons has been described by the Lindhard function [23].

For a first attempt to estimate the magnitude of RM corrections it is appropriate to look at insulating materials, where all target electrons may be considered as bound. Fig. 2 shows comparisons between uncorrected, RM1- and RM2-corrected stopping cross sections for H, He and N ions in Ne as well as H, C and Ar ions in Ar[1].

It is seen that RM corrections are very small at energies above 10 keV/u but increase significantly with decreasing energy. The biggest values are found for H ions, where PASS predicts an order-of-magnitude decrease which may be considered as an effective threshold effect.

Experimental values extracted from ref. [32] have been included in the graphs, but none of these data sets includes the energy range where a measurable RM correction can be expected. Note that the pronounced change in slope for N-Ne in data from ref. [28] has been found [33] to result from an incorrect nuclear-stopping correction.

Measurements at beam energies down to below 1 keV/u have been performed on solid materials. Here, care needs to be taken of the presence of free or weakly-bound electrons, where the assumption of coupling between electronic excitation by and angular deflection of the projectile becomes questionable. For a free electron gas, electronic and nuclear interactions may be taken to be strictly independent from each other. Consequently, RM corrections are applied to bound electrons, while no correction is applied to free-electron shells.

[1] Sources of experimental data for low beam energies $E \lesssim 20$ keV/u are quoted explecitly in the following. Other data have been extracted from ref. [32]

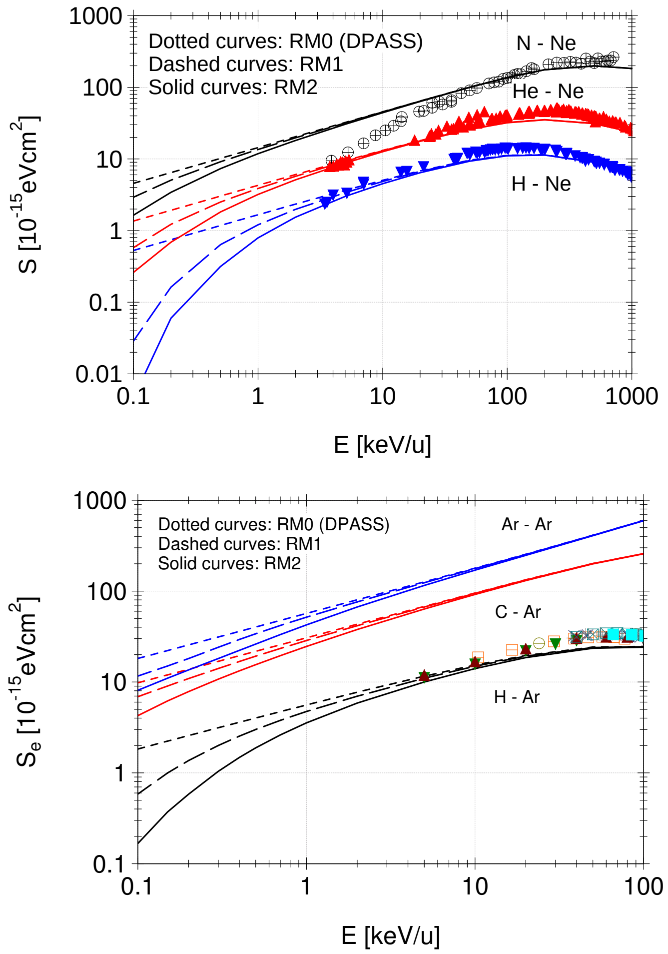

Figure 2: RM correction applied to stopping in Ne (upper graph) and Ar (lower graph). Low-energy data from refs. [24, 25, 26, 27, 28] for Ne target and refs. [29, 30, 31] for Ar target. See text.

This leaves open the question of where to place the borderline between free and bound electrons. While several criteria are available, such as chemical valence or the magnitude of shell binding energies, we may actually treat the magnitude of RM corrections as a tool to distinguish between free and bound electrons.

Examples were presented in ref. [3], where the uncontroversial choice of one free electron per target atom produced good agreement between measured and RM-corrected stopping cross sections for Cu, Ag and Au, while for H in Ni, adoption of 11 free electrons per target atom, i.e., treating the outermost 2 shells as free electrons, was found to produce better agreement with measured stopping cross sections than just the outermost shell.

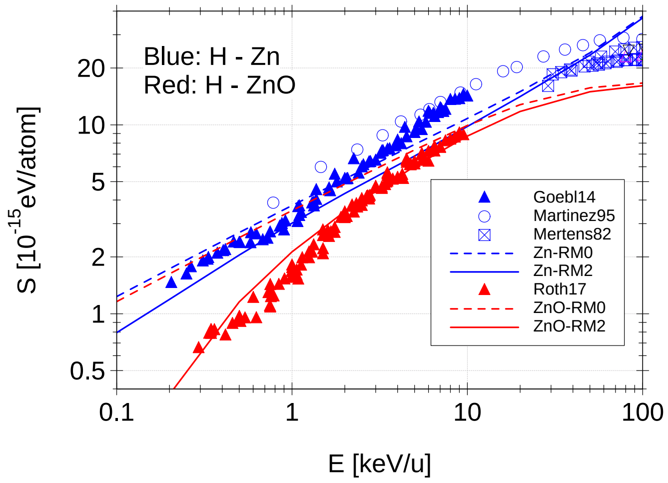

Figure 3: RM correction applied to stopping of H ions in Zn and ZnO. For clarity, only RM0 and RM2 are shown.

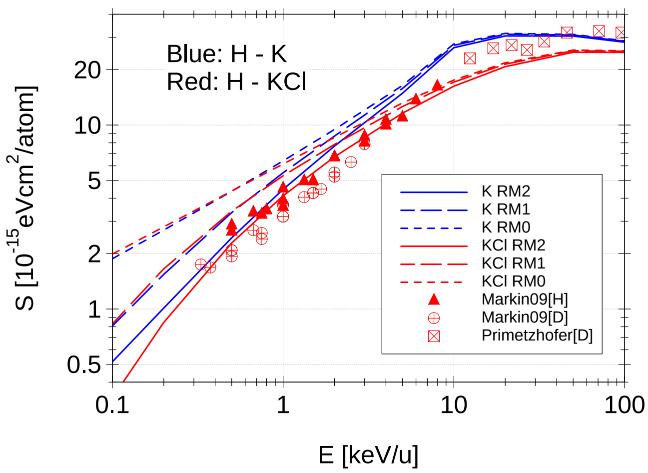

Figure 4: Stopping cross sections measured for KCl compared with uncorrected and RM-corrected stopping cross sections calculated by PASS.

Figure 3 shows a comparison of measured with calculated stopping cross sections for H ions in Zn and ZnO. ZnO, as well as other compound materials to be discussed in the following, are here characterized by a routine described in ref. [34], which involves rearrangement of the target electrons between the components. In case of ZnO this implies that the I-values and binding energies of the two 4s electrons in Zn are assigned to the 2p shell of oxygen. In this way, ZnO has only filled shells. Stopping cross sections are then found by assuming Bragg additivity to this configuration.

Theoretical curves for Zn show a moderate RM2 correction, based on the assumption of 2 free electrons per atom, which would be even smaller if we had chosen 12, i.e., the two outermost electron shells. There is found good agreement between calculated and measured stopping cross sections and a clear conductor-insulator difference, as evidenced by a pronounced difference in slope in the low-energy regime.

A similar result was found [3] in a comparison between the H-Si and H-SiO_2 systems, which demonstrated that with respect to electronic stopping, the semiconductor silicon behaves more like a conductor than like an insulator.

Figures. 4 and 5 show similar graphs for KCl and three transition metal oxides. There is found good agreement between calculated and measured data for all four compounds, in particular in the predicted difference in slope from the uncorrected curves. For the pure metals, good agreement is found for V and Hf, but those data do not extend into the low-energy regime. The rather high value for Ta – which has been reported from two independent sources [37, 36] – appears surprising, considering the behavior of the oxide.

4. Stopping measurement

Stopping cross sections for low-energy ions are mostly measured in transmission or reflection geometry or extracted from range measurements. Our discussion of reflection data in ref. [3] has demonstrated good agreement with measurements especially for H ions in Au, Ag, Cu and Ni on the basis of simulations with the OKSANA code [2], incorporating impact-parameter-dependent energy losses predicted by PASS.

Measurements in transmission geometry have been discussed in ref. [1] as an extension of the standard theory for the nuclear-stopping correction [38]. As sketched in Fig. 6, ions get scattered while passing the target foil, with the result that the energy distribution of ions hitting the detector differs from what would be expected if deflection were neglected. In the friction model of electronic energy loss, scattering only affects nuclear stopping [38]. Incorporating the impact-parameter dependence of electronic energy loss implies a decrease also of the electronic energy loss recorded by the detector.

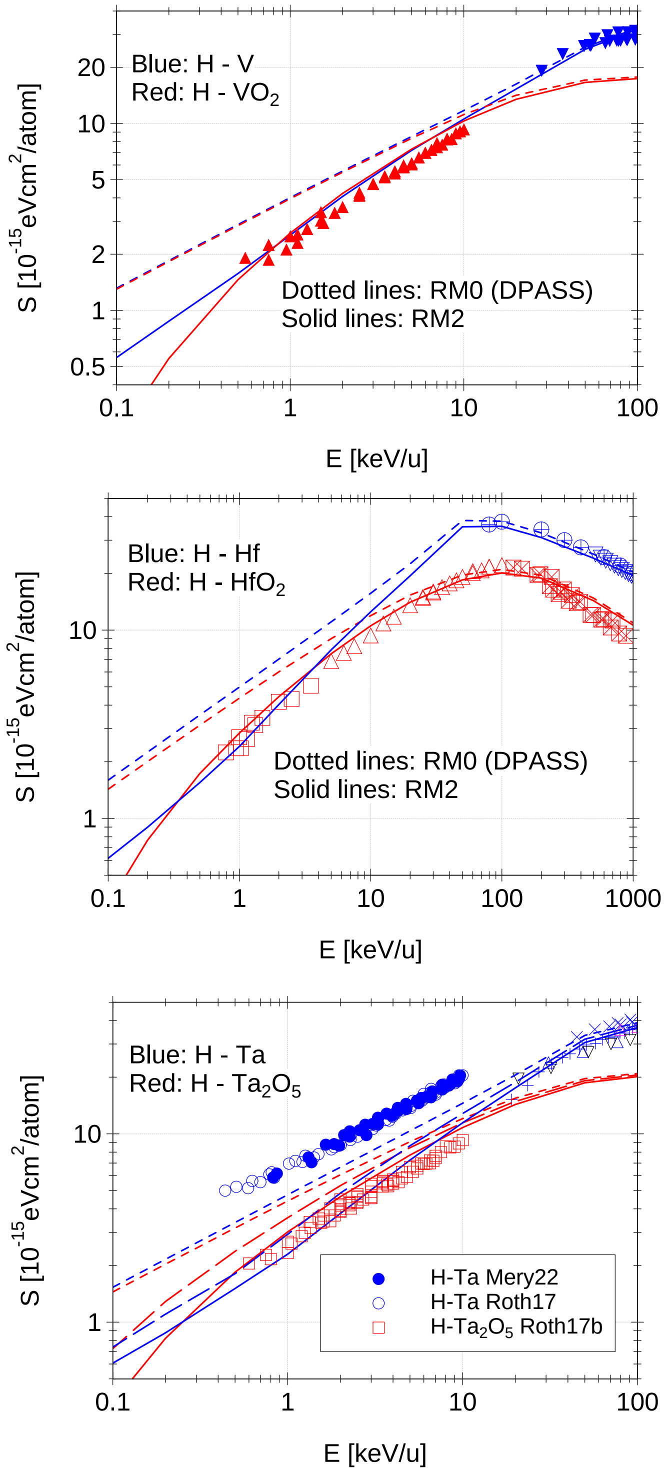

Figure 5: Same as Fig. 3 for V, Hf, Ta and the corresponding oxides. Experimental data from ref. [35] for VO_2 HfO_2 and Ta_2O_3, refs. [36, 37] for Ta.

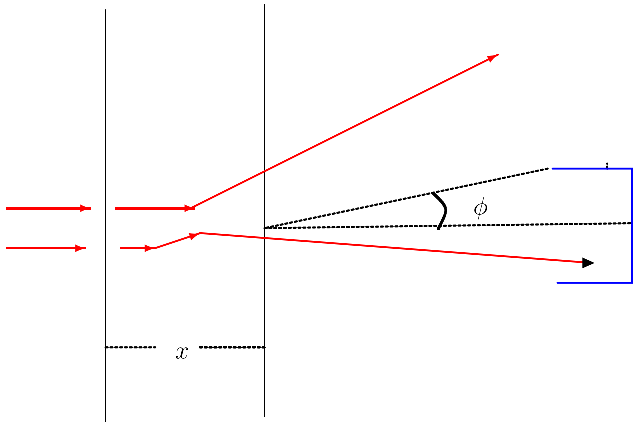

Figure 6: Stopping measurement in transmission. See text.

A proper treatment of this effect requires due account of multiple scattering. Such a treatment was presented in ref. [1], based on Bohr-Williams theory of multiple scattering [5]. The resulting reduction of the measured signal was termed RED correction. We concluded that stopping cross sections measured in transmission had to be larger than reported, when corrected only for nuclear stopping.

However, these calculations did not incorporate an RM correction. Since it is the same collisions that lead to both RED and RM corrections, we cannot expect linear superposition. Instead, the substitution of the impact parameter p by the distance of closest approach RM as well as the change in instantaneous energy must be made in the multiple-scattering description of the penetration through the target foil.

Figure 7 shows the result of this treatment for H-Au and H-Ag. These graphs represent expanded versions of figs. 5 and 6 in ref. [3]: Blue lines represent 'true' RM-corrected stopping cross sections reported in ref. [3], whereas red lines indicate what is expected to be measured in a transmission experiment with detector opening angle and foil thickness reflecting experimental conditions reported in ref. [39]. Here, the difference between the blue RM0 line and the red RM0 line reflects the RED correction treated in ref. [1], which is found to be quite small.

Comparison between the two RM2 lines shows that the effect of the RM correction is *smaller* in the signal measured in transmission than in the true stopping cross section. This is to be expected, since both scattering angle and energy loss in single collisions are smaller when the impact parameter has increased from p to R_{min}.

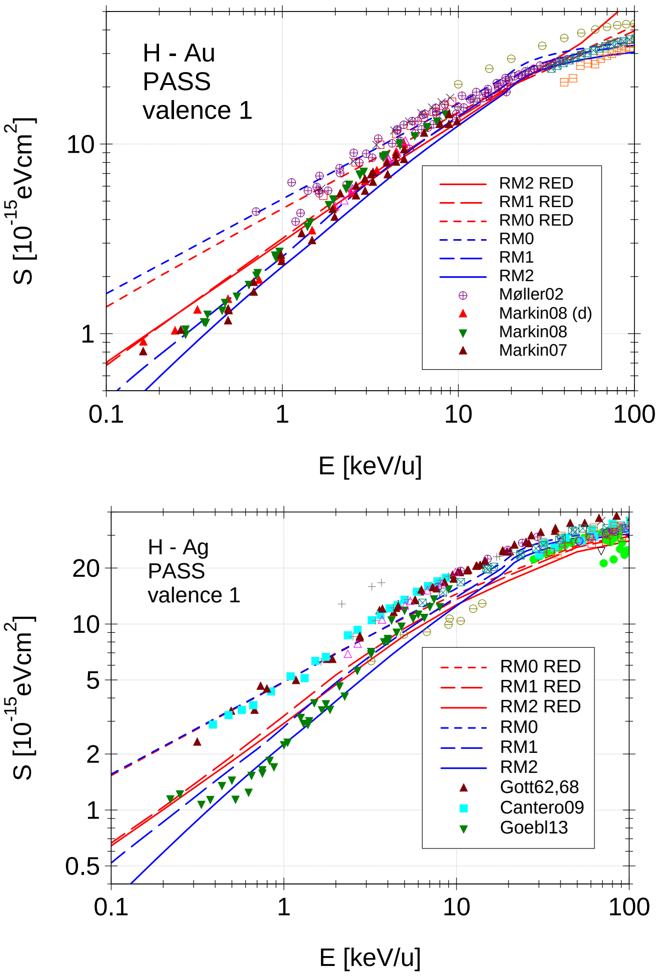

Figure 7: Apparent stopping cross section of H in Au (upper graph) and Ag (lower graph) in transmission experiment. Foil thickness and detector opening angle taken as reported in ref. [39]. See text.

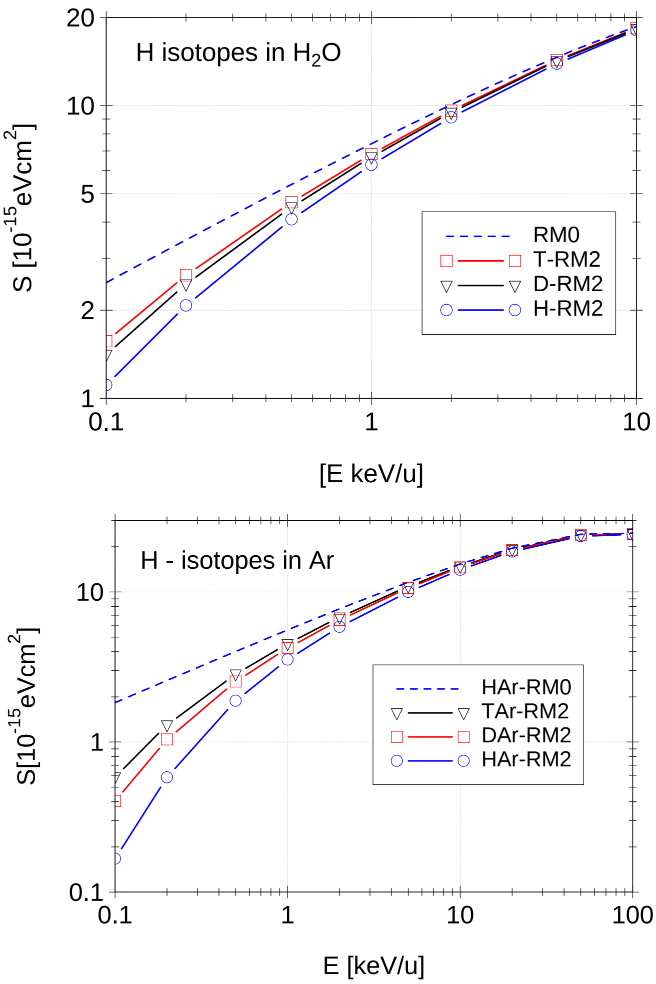

Figure 8: Uncorrected and RM-corrected electronic stopping cross sections for H, D and T ions in Argon (upper graph) and H_2O (lower graph).

5. Isotope Effect

Since elastic scattering depends on the nuclear masses of the collision partners, RM- as well as RED-corrected stopping cross sections are expected to show an isotope effect. Experimental evidence was presented in ref. [3] by comparing stopping cross sections for H-Si and D-Si from ref. [40].

Measurements with deuterons are commonly performed with the aim to extend the velocity range of hydrogen ions toward lower values. Although this equivalence is usually tested, measurements tend to be done at energies where the isotope effect is small. A key point must be the separation of nuclear stopping.

In view of the smallness of the isotope effect, strong evidence might be best searched in measurements on insulators. Figure 8 shows estimates of stopping cross sections in H_2O and Ar for H, D and T ions. It is seen that for both materials, measurements at around 1 keV/u or lower should reveal a clear result.

6. Summary

- This study confirms the significance of RM corrections for light ions at low beam energies, $E \lesssim 20$ keV/u.
- We have not reported results for heavier ions, mainly because measurements at low energies are sparse. But for this very reason, theoretical results based on an established model may become useful.
- We find it necessary to include the impact-parameter dependence or an equivalent in a valid description of electronic stopping in the considered energy range. Evidently, in a fully quantal description, this effect is contained from the start. On the other hand, frequently-used semiquantal descriptions, where nuclear motion follows classical scattering while electronic motion is described quantally, RM corrections need to be added explicitly.
- In addition to the projectile charge, also the projectile mass affects electronic stopping.
- The magnitude of the RM correction is smaller in the signal delivered in a transmission measurement than in the stopping cross section.
- The magnitude of the RM correction may serve as a qualitative indicator of the borderline between inner and outer electrons with regard to their significance in the stopping cross section.

References

[1] P. Sigmund and A. Schinner, Nucl. Instrum. Methods B 410 (2017) 78.
[2] V. I. Shulga, A. Schinner and P. Sigmund, Nucl. Instrum. Methods B 467 (2020) 91.
[3] A. Schinner, V. Shulga and P. Sigmund, J. Appl. Phys. 129 (2021) 183304.
[4] N. Bohr, Philos. Mag. 25 (1913) 10.
[5] N. Bohr, Mat. Fys. Medd. Dan. Vid. Selsk. 18 no. 8 (1948) 1.
[6] J. Lindhard and M. Scharff, Phys. Rev. 124 (1961) 128.
[7] J. Lindhard, M. Scharff and H. E. Schiøtt, Mat. Fys. Medd. Dan. Vid. Selsk. 33 no. 14 (1963) 1.
[8] J. Lindhard, V. Nielsen, M. Scharff and P. V. Thomsen, Mat. Fys. Medd. Dan. Vid. Selsk. 33 no. 10 (1963) 1.
[9] J. F. Ziegler, J. P. Biersack and U. Littmark, *The stopping and range of ions in solids*, vol. 1 (Pergamon, New York, 1985).
[10] P. Sigmund, *Particle Penetration and Radiation Effects Volume 2*, vol. 179 of *Springer Series in Solid State Sciences* (Springer, Heidelberg, 2014).
[11] P. Sigmund and A. Schinner, Nucl. Instrum. Methods B 195 (2002) 64.
[12] A. Schinner and P. Sigmund, *DPASS stopping code* (2020), https://www.sdu.dk/en/forskning/fysik/forskere/kvanteoptik/peter-sigmund/dpass.
[13] P. L. Grande and G. Schiwietz, Nucl. Instrum. Methods B 195 (2002) 55.
[14] *CasP version 6.0* (2021), `http://www.casp-program.org/`.
[15] H. Bethe, Ann. Physik 397 no. 3 (1930) 325.
[16] O. B. Firsov, Zh. Eksp. Teor. Fiz. 36 (1959) 1517, [Engl. transl. Sov. Phys. JETP **9**, 1076-1080 (1959)].
[17] H. Goldstein, *Classical mechanics* (Addison-Wesley Press, Cambridge, Mass., 1953).
[18] J. Bang and J. Hansteen, Mat. Fys. Medd. Dan. Vid. Selsk. 31 no. 13 (1959) 1.
[19] Y. A. Teplova, V. S. Nikolaev, I. S. Dimitriev and L. N. Fateeva, Zh. Eksp. Teor. Fiz. 42 (1962) 44, [Engl. transl. Sov. Phys. JETP **15**, 31-41 (1962)].
[20] D. S. Karpuzov, Appl. Phys. 24 (1981) 121.
[21] D. Semrad, Phys. Rev. A 33 (1986) 1646.
[22] E. Fermi and E. Teller, Phys. Rev. 72 (1947) 399.
[23] J. Lindhard, Mat. Fys. Medd. Dan. Vid. Selsk. 28 no. 8 (1954) 1.
[24] A. Schiefermüller, R. Golser, R. Stohl and d. Semrad, Phys. Rev. A 48 (1993) 4467.
[25] D. Jedrejcic and U. Greife, Nucl. Instrum. Methods B 428 (2018) 1.
[26] P. Hvelplund, Mat. Fys. Medd. Dan. Vid. Selsk. 38 no. 4 (1971) 1.
[27] J. L. Price, D. G. Simons, S. H. Stern, D. J. Land, N. A. Guardala, J. G. Brennan and M. F. Stumborg, Phys. Rev. A 47 (1993) 2913.
[28] A. Fukuda, J. Phys. B 29 (1996) 3717.
[29] J. A. Phillips, Phys. Rev. 90 (1953) 532.
[30] R. I. Wolke, W. N. Bishop, E. Eicher, N. R. Johnson and G. D. O'Kelley, Phys. Rev. 129 (1963) 2591.
[31] J. H. Ormrod, Can. J. Phys. 46 (1968) 497.
[32] *Electronic Stopping Power of Matter for Ions* (2020), `https://www-nds.iaea.org/stopping/`.
[33] P. Sigmund and A. Schinner, Nucl. Instrum. Methods B 440 (2019) 41.
[34] P. Sigmund and A. Schinner, Nucl. Instrum. Methods B 415 (2018) 110.
[35] D. Roth, B. Bruckner, G. Undeutsch, V. Paneta, A. I. Mardare, C. I. McGahan, M. Dosmailov, J. I. Juaristi, M. Alducin, J. D. Pedarnig, R. F. Haglund, D. Primetzhofer and P. Bauer, Phys. Rev. Lett. 119 (2017) 163401.
[36] M. Mery, L. Chen, J. E. Valdes and V. A. Esaulov 175 (2022) 160.

[37] D. Roth, B. Bruckner, M. V. Moro, S. Gruber, D. Goebl, J. I. Juaristi, M. Alducin, R. Steinberger, J. Duchoslav, D. Primetzhofer and P. Bauer, Phys. Rev. Lett. 118 (2017).
[38] B. Fastrup, P. Hvelplund and C. A. Sautter, Mat. Fys. Medd. Dan. Vid. Selsk. 35 no. 10 (1966) 1.
[39] E. D. Cantero, R. C. Fadanelli, C. C. Montanari, M. Behar, J. C. Eckardt, G. H. Lantschner, J. E. Miraglia and N. R. Arista, Phys. Rev. A 79 (2009) 042904.
[40] G. Konac, S. Kalbitzer, C. Klatt, D. Niemann and R. Stoll, Nucl. Instrum. Methods B 138 (1998) 159.